



Preliminary Monte Carlo and Thermal Hydraulic Analysis using a Hybrid ETF-Corrected-Diffusion Prediction Block

August 2023

Changing the World's Energy Future

Bailey Painter, Stefano Terlizzi, Dan Kotlyar



INL is a U.S. Department of Energy National Laboratory operated by Battelle Energy Alliance, LLC

DISCLAIMER

This information was prepared as an account of work sponsored by an agency of the U.S. Government. Neither the U.S. Government nor any agency thereof, nor any of their employees, makes any warranty, expressed or implied, or assumes any legal liability or responsibility for the accuracy, completeness, or usefulness, of any information, apparatus, product, or process disclosed, or represents that its use would not infringe privately owned rights. References herein to any specific commercial product, process, or service by trade name, trade mark, manufacturer, or otherwise, does not necessarily constitute or imply its endorsement, recommendation, or favoring by the U.S. Government or any agency thereof. The views and opinions of authors expressed herein do not necessarily state or reflect those of the U.S. Government or any agency thereof.

Preliminary Monte Carlo and Thermal Hydraulic Analysis using a Hybrid ETF-Corrected-Diffusion Prediction Block

Bailey Painter, Stefano Terlizzi, Dan Kotlyar

August 2023

**Idaho National Laboratory
Idaho Falls, Idaho 83415**

<http://www.inl.gov>

**Prepared for the
U.S. Department of Energy
Under DOE Idaho Operations Office
Contract DE-AC07-05ID14517**

Preliminary Monte Carlo and Thermal Hydraulic Analysis using a Hybrid ETF-Corrected-Diffusion Prediction Block

Bailey Painter¹, Dan Kotlyar¹, and Stefano Terlizzi²

¹Georgia Institute of Technology
770 State St NW, Atlanta, GA 30313

²Idaho National Laboratory
1955 N Fremont Ave, Idaho Falls, ID 83415,
painter@gatech.edu, stefano.terlizzi@inl.gov, dan.kotlyar@me.gatech.edu

ABSTRACT

This paper builds upon previous work to accelerate the Picard iteration (PI) method typically applied for coupled Monte Carlo-Thermal hydraulic (MC-TH) solutions. Previously, the use of the generalized transfer functions (GTFs) to predict variation in macroscopic cross sections following a perturbation in TH properties was demonstrated for a subset of simple 3D problems. In addition, the reduced-order transport prediction block relied on the first order perturbation (FOP) method, which was shown to have computational overheads. Recent work replaced the FOP block with a 1-group nodal diffusion solver to eliminate these overheads. While the use of diffusion is desirable for large-scale problems, the new solver introduces significant homogenization error. This work aims to address this issue by using the Jacobian-Free Newton Krylov (JFNK) method to generate a set of super homogenization (SPH) factors to improve the accuracy of the diffusion solution. The SPH factors will be used in conjunction with an improved cross section prediction method – the expanded transfer function (ETF) method – to produce a highly accurate flux prediction for an axial 1D boiling water reactor (BWR) pincell following a large perturbation in moderator density. The ETF-corrected diffusion (ETF-CD) block is shown to be highly accurate for the 1D test case. Future work will investigate the accuracy of the method for a realistic 3D pressurized water reactor core.

KEYWORDS: Multiphysics, Monte Carlo, Thermal Hydraulics, Transfer Functions, Cross sections

1. INTRODUCTION

The Picard iteration (PI) scheme is the most widely used technique to couple Monte Carlo (MC) neutronic codes to Thermal hydraulic (TH) codes. Although the PI scheme is typically straightforward in its implementation the scheme has only linear convergence rate at best. In essence, the PI scheme requires the MC and TH codes to be executed multiple times in a series until the neutronic and TH fields converge. To accelerate the PI convergence, the general approach is to use a reduced order neutronic model [1, 2, 3, 4, 5]. This method has two distinct benefits: (1)

it allows for the removal of inactive cycles and (2) it introduces greater flexibility for determining the number of particles vs active cycles; thus, making the simulation more parallelizable. In our previous work, Ref. [2], the acceleration was performed in two sub-blocks. In the first subblock, generalized transfer functions (GTFs) were used to predict the response of 1-group, macroscopic cross sections to changes in fuel temperature and moderator/coolant density [3, 4]. In the second sub-block, first order perturbation (FOP) theory was used to estimate the response of the multiplication factor and source profile to the change in the group constants.

In the FOP sub-block, the fission matrix from a previous MC solution is used to calculate the eigenvalues and eigenvectors of the source. The main drawback of the GTF-FOP method is that the fission matrix is computationally expensive to obtain. Recent work has shown that the computational overheads can be greatly reduced if a nodal diffusion solver is used instead. Previously, the authors implemented GTF-Nodal Diffusion (GTF-ND) in Ref. [5] and demonstrated the sequence for a 1D boiling water reactor (BWR) pincell with uniform enrichment. The transfer function approach was built upon by introducing the expanded transfer function (ETF) method which was demonstrated on the 1D BWR pincell in Ref. [6].

While cross section prediction is highly accurate with the novel ETF method, there still exists a homogenization error in the nodal diffusion solution that needs to be addressed. This error was shown to be small for the 1D BWR pincell in Ref. [5], but ongoing work has observed that the error is significantly more prominent in 3D cases. This paper will investigate the application of super homogenization (SPH) factors to introduce a simple correction to the diffusion solution. These SPH factors will be obtained using the Jacobian-free Newton Krylov (JFNK) method, which has been shown to be a fast and reliable method to produce these factors [7]. This new prediction block will be referred to as the ETF-corrected diffusion (ETF-CD) block. Future work will investigate the application of the ETF-CD block to the realistic 3D pressurized water reactor (PWR) core in Ref. [8]. There is also ongoing work focused on the generation of correction factors with the JFNK for the PWR core [9].

Like in Ref. [5], the explicit flux in the BWR pincell is solved using the continuous energy MC code Serpent and the reduced-order flux is solved using the multigroup ND solver DYN3D [10,11]. SPH factors are generated using the JFNK method (detailed in section 2.2) and are used to match the initial homogenous solution (DYN3D) to the initial heterogenous solution (Serpent). The ETF method is used to create a linear response model of each macroscopic cross section. This model is then used with a perturbed coolant density distribution to predict a corresponding set of cross sections (for simplicity, no perturbations in fuel temperature are investigated in this paper). The correction factors and predicted, perturbed cross sections are fed to DYN3D to calculate the new k_{eff} and power distribution. These results are compared against the Serpent-generated perturbed flux and a good agreement is observed.

2. METHODOLOGY AND IMPLEMENTATION

This section describes the methods used in the ETF-CD block. Section 2.1 describes the super homogenization (SPH) factors that will be used to correct the nodal diffusion solution. Section 2.2 describes the JFNK method that will be used to produce the correction factors. Section 2.3

will describe the overall workflow of the ETF-CD corrected diffusion block. Finally, Section 2.4 describes the figures of merit used to quantify error in this study.

2.1. SPH factors

Super homogenization (SPH) factors were introduced in Ref. [12] and were later expanded by Ref. [13]. SPH Factors adjust the balance equation within a node (Eq. 1) by introducing a correction factor $\mu(i)$ for node i (Eq. 2). Since SPH factors change the homogenous solution, these factors must be calculated iteratively to satisfy the definition in Eq. 2 as closely as possible.

$$-\mu(i)D(i)\nabla^2\phi(i) + \mu(i)\Sigma_a(i)\phi(i) = \frac{1}{k}\mu(i)v\Sigma_f(i)\phi(i) \quad (1)$$

$$\mu(i) \approx \frac{\phi_{het}(i)}{\phi_{hom}(i)} \quad (2)$$

It is also custom to apply SPH factors to minimize the error of the homogeneous k_{eff} . This is an undesirable minimization objective for this work since k_{eff} is an integral quantity and may not actually be indicative of how well the spatial flux distribution is conserved. This emphasizes the need for the JFNK which can be used to minimize the error on the spatial flux distribution.

2.2. JFNK method

The application of the JFNK to calculate SPH factors was first investigated by Ref [7] and the methods used in this paper are largely similar. The JFNK method is used to find a set of SPH factors \mathbf{x} that minimizes the residual error $F(\mathbf{x})$ between a corrected nodal diffusion solution $\phi_{hom}(\mathbf{x})$ and a known heterogenous solution ϕ_{het} (Eq. 3). The JFNK is performed in a series of inner and outer iterations. The outer Newton Raphson iterations begin with an initial guess of the correction factors \mathbf{x}_0 that is close to the root of $F(\mathbf{x})$. The correction factors are updated each Newton iteration by using a first-order Taylor expansion of $F(\mathbf{x})$ (Eq. 4). $J(\mathbf{x}_i)$ is the Jacobian at the i^{th} iteration and $\delta\mathbf{x}_i$ is the approximated change in each correction factor at iteration i to minimize $F(\mathbf{x}_{i+1})$.

$$F(\mathbf{x}) = \phi_{hom}(\mathbf{x}) - \phi_{het} \quad (3)$$

$$F(\mathbf{x}_{i+1}) \approx F(\mathbf{x}_i) + J(\mathbf{x}_i)\delta\mathbf{x}_i \quad (4)$$

2.2.1. FGMRES

The most straightforward approach to finding the $\delta\mathbf{x}$ is to apply the regression formula in Eq. 5. However, J depends on the response of a nonlinear nodal diffusion solution to a change in SPH factors. J is therefore impossible to calculate analytically and computationally expensive to approximate numerically. The standard JFNK approach relies on general minimum residual (GMRES) methods which can approximate $\delta\mathbf{x}$ without needing to calculate J . This paper specifically relies on the flexible generalized minimum residual (FGMRES) method [15] to

obtain the approximate solution $\delta \mathbf{x}_n$. The main idea of FGMRES is that $\delta \mathbf{x}_n$ is approximated to exist in the subspace Z_n which is spanned by a set of arbitrary orthogonal basis vectors $[\mathbf{z}_1, \mathbf{z}_2, \dots, \mathbf{z}_n]$ (Eq. 6). As discussed below, this arbitrary subspace can accommodate constraints to $\delta \mathbf{x}_n$ that the standard GMRES method cannot.

$$\delta \mathbf{x} = \mathbf{J}^{-1} \mathbf{F}(\mathbf{x}) \quad (5)$$

$$\delta \mathbf{x}_n \in Z_n = [\mathbf{z}_1, \mathbf{z}_2, \dots, \mathbf{z}_n] \quad (6)$$

The full derivation of the FGMRES will be discussed in Ref. [9]. Briefly, each Jacobian-vector product $[\mathbf{J}\mathbf{z}_1, \mathbf{J}\mathbf{z}_2, \dots, \mathbf{J}\mathbf{z}_n]$ is approximated using the finite difference formula in Eq. 7, where ϵ is a small number (0.1 in this paper). Each product establishes a new vector in the subspace Q_{n+1} . This relationship between Z_n and Q_{n+1} is known as the partial similarity transform in Eq. 9 where \tilde{H}_n is an upper Hessenberg matrix.

$$\mathbf{J}\mathbf{z}_k \approx \frac{F(\mathbf{x}_i + \epsilon \mathbf{z}_k) - F(\mathbf{x}_i)}{\epsilon} \quad (7)$$

$$Q_{n+1} = [\mathbf{q}_1, \mathbf{q}_2, \dots, \mathbf{q}_{n+1}] \quad (8)$$

$$\mathbf{J}Z_n = \tilde{H}_n Q_{n+1} \quad (9)$$

The basis vectors $[\mathbf{z}_1, \mathbf{z}_2, \dots, \mathbf{z}_k]$ are typically closely related to $[\mathbf{q}_1, \mathbf{q}_2, \dots, \mathbf{q}_k]$. In fact, the relationship $\mathbf{z}_k = \mathbf{q}_k$ results in the standard GMRES procedure. In this study, SPH factors must be constrained to be positive so the relationship between \mathbf{z}_k and \mathbf{q}_k is altered slightly. Here, an intermediate vector \mathbf{z}'_k is first calculated. $\mathbf{z}'_k(i) = 0$ if the SPH factor in region i is close to 0 and $\mathbf{z}'_k(i) = \mathbf{q}_k(i)$ otherwise. \mathbf{z}_k is then the component of \mathbf{z}'_k that is orthogonal to the subspace Z_{k-1} .

The Arnoldi process stops when one of three conditions is met: $\mathbf{q}_k = \vec{0}$, $\mathbf{z}_k = \vec{0}$, or the number of user specified Arnoldi iterations n has completed. Upon completion, the output \tilde{H}_n and Z_n are used to calculate $\delta \mathbf{x}_n$. The partial similarity transform is used to establish the minimization problem in Eq. 10. Solving this gives a set of coefficients \mathbf{y}_n that can be used with Eq. 11 to obtain $\delta \mathbf{x}_n$. Another FGMRES iteration or “restart” could be executed to further minimize $F(\mathbf{x}_{i+1})$. In this study, only a single FGMRES iteration is performed each Newton iteration. An overview of the JFNK algorithm used in this paper is detailed in Fig. 1.

$$\min \|F(\mathbf{x}_{i+1})\| = \min \|\tilde{H}_n \mathbf{y}_n - \|F(\mathbf{x}_i)\|_2 \mathbf{e}_1\| \quad (10)$$

$$\delta \mathbf{x}_i \approx Z_n \mathbf{y} \quad (11)$$

1. Choose initial guess \mathbf{x}_0
2. For $i = 1, 2, \dots$
 - a. Calculate $\tilde{\mathbf{H}}_n, \mathbf{Z}_n$ using n Arnoldi iterations.
 - b. Solve the minimization: $\min \|\tilde{\mathbf{H}}_n \mathbf{y} - \|F(\mathbf{x}_i)\|_2 \mathbf{e}_1\|$
 - c. Update \mathbf{x} : $\mathbf{x}_{i+1} = \mathbf{x}_i + \delta \mathbf{x}_i$
Where: $\delta \mathbf{x}_i = \mathbf{Z}_n \mathbf{y}$
 - d. Check convergence: if $F(\mathbf{x}_{i+1}) > F(\mathbf{x}_i)$ then break and return \mathbf{x}_i . Otherwise, continue.

Figure 1. JFNK algorithm applied in this paper.

2.3. ETF-CD prediction block

For the complete ETF theory, please refer to Ref. [6].

1. *Initial conditions*: The TH solver produces an initial spatial distribution of the moderator density $\bar{\rho}^{(0)}$ which is fed to the MC code to obtain one-group¹ macroscopic cross sections $\bar{\Sigma}_x^{(0)}$ and the power $\bar{P}^{(0)}$.
2. *Correction factor calculation*: The JFNK method is used with DYN3D to generate a set of correction factors \bar{f}_c that allow the DYN3D solution to closely match the initial serpent solution when using the initial cross sections. $\bar{\Sigma}_x^{(0)}$.
3. *ETF Model*: An initial ETF model $\bar{\bar{A}}^{(0)}$ is calculated. $\bar{\bar{A}}^{(0)}$ is a matrix and each column represents a property at a specific distance away. In this paper, $\bar{\bar{A}}^{(0)}$ contains three properties: the initial moderator density $\bar{\rho}^{(0)}$, the presence of reflectors, and the presence of fuel. $\bar{\bar{A}}^{(0)}$ contains these three inputs at distances of 0, 1, 2, and 3 axial layers away. $\bar{\bar{A}}^{(0)}$ also contains a column representing an intercept term to stabilize the model. In total, there are 13 columns in $\bar{\bar{A}}^{(0)}$.
4. *ETF Calculation*: Expanded Transfer Functions \bar{w}_x for each macroscopic cross section x by performing a linear regression on the linear system in equation 1. \bar{w}_x is a vector that represents the weight applied to each property at specific distance away to construct a prediction of Σ_x :

$$\bar{\bar{A}}^{(0)} \bar{w}_x = \bar{\Sigma}_x^{(0)} \quad (12)$$

5. *TH prediction*. The TH solver calculates $\bar{\rho}^{(1)}$ using $\bar{P}^{(0)}$ as an input.

¹ The cross sections used in this workflow are required by the nodal-diffusion code DYN3D. These include the reduced-order absorption, fission, nu-fission, kappa-fission, and transport cross section.

6. *ETF prediction.* A perturbed ETF model $\bar{A}^{(1)}$ is calculated in the same way as $\bar{A}^{(0)}$ using $\bar{\rho}^{(1)}$ instead of $\bar{\rho}^{(0)}$. This perturbed model is used with \bar{w}_x to predict each macroscopic cross section in the perturbed state.

$$\bar{\Sigma}_x^{(1)} \approx \bar{A}^{(1)} \bar{w}_x \quad (13)$$

7. *ND Solver:* The correction factors \bar{f}_c calculated in step 2 and the predicted, perturbed cross sections $\bar{\Sigma}_1(x)$ calculated in step 6 are fed to DYN3D to obtain a predicted, perturbed spatial power distribution $P_1(x)$ and eigenvalue k_1 .

8. *Results:* $P_1(x)$ and k_1 are fed into the MC solver as an improved initial guess for the source in the next iteration.

The TH code THERMO is used to compute density profiles for given power profiles [14]. serpentTools was used to read and automatically store cross section data from Serpent output files [16].

2.4. Figures of Merit

Three figures of merit (FOM) are used in this paper. The L2 percent error (*L2PE*) in Eq. 14 quantifies the error in flux between a homogenous solution and a known heterogenous solution. The reactivity deviation ($\Delta\rho$) in Eq. 15 quantifies the error in k_{eff} in pcm between a homogeneous and heterogenous solution. Finally, the mean absolute percent error (*MAPE*) in Eq. 16 quantifies the error between an ETF-predicted cross section and a known cross section produced by Serpent.

$$L2PE = \frac{\|\phi_{hom} - \phi_{het}\|_2}{\|\phi_{het}\|_2} \times 100\% \quad (14)$$

$$\Delta\rho = \left| \frac{1}{k_{hom}} - \frac{1}{k_{het}} \right| \times 10^5 \text{ pcm} \quad (15)$$

$$MAPE = \frac{1}{N} \left(\sum_{i=1}^N \left| 1 - \frac{\Sigma_{hom}(i)}{\Sigma_{het}(i)} \right| \right) \times 100\% \quad (16)$$

3. RESULTS

These results are a preliminary demonstration of the ETF-CD prediction block to produce accurate solutions using the results of a single heterogenous calculation. Section 3.1 details the process used to calculate the correction factors using a known, reference solution. Section 3.2 details the results of the ETF prediction of each cross section. Section 3.3 shows the result of the ETF-CD prediction and explores which correction factors are most suitable for the prediction.

3.1. Reproducing Serpent CE results with DYN3D MG

The first part of this benchmark will be to calculate SPH factors for the DYN3D homogenous solution. The $L2PE$ between Serpent and DYN3D in the initial state is 1.48%. A large portion of this error is towards the peak of the flux which is lower in the DYN3D solution as shown in Fig. 2. SPH factors were obtained using both low rank approximation (10 Arnoldi iterations) and a full rank calculation (38 Arnoldi iterations) of $\delta\mathbf{x}$. The axial distributions the SPH factors for each case is shown in Fig. 3. The homogenous solution corrected with full-rank SPH factors is shown in Fig. 2. The full rank SPH factors were significantly better at correcting errors in the DYN3D solution. In fact, the $L2PE$ for the low rank approximation saturated to a higher level of error. The ability of SPH factors to correct a homogenous solution appears to depend heavily on the number of Arnoldi iterations used at each Newton step. This could be problematic for larger problems if no preconditioning is applied.

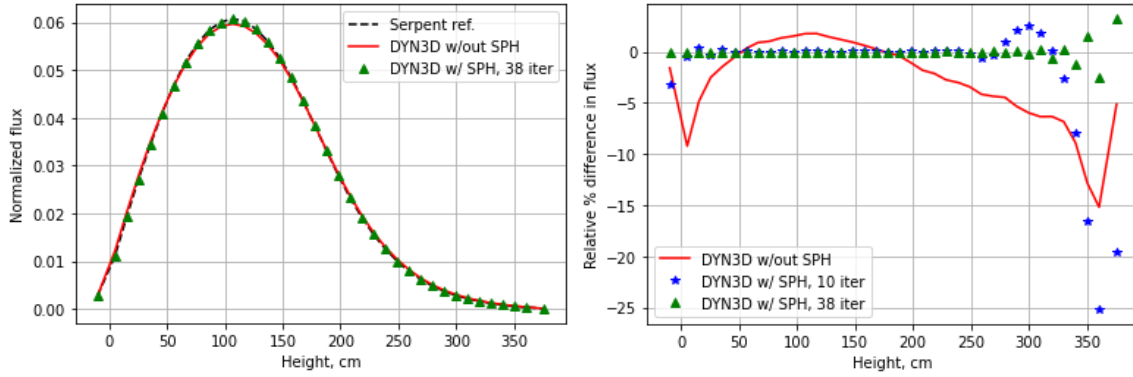


Figure 2. Normalized heterogenous and homogenous flux (left) and relative % error between heterogenous and homogenous flux (right) for the reference state.

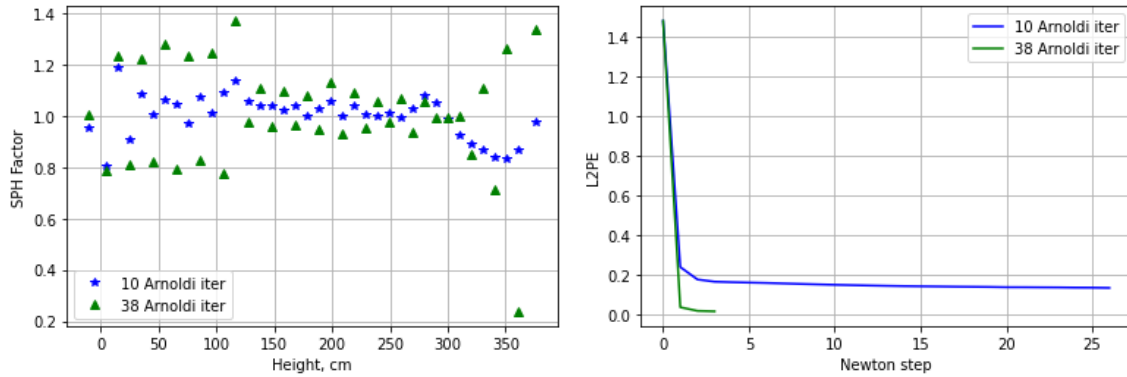


Figure 3. Calculated SPH factors (left) and the evolution of the homogenous error with each Newton step (right)

Table I. Flux and k_{eff} errors for the initial state

	# Arnoldi steps	Newton Steps	$L2PE$ (%)	$\Delta\rho$ (pcm)
Uncorrected	--	--	1.48	19
SPH	10	26	0.132	12
	38	3	0.0137	11

3.2. Prediction of perturbed cross sections

The second benchmark explores the ability of the ETF method to predict each one-group cross section. Fig. 4 shows the moderator density for the initial and perturbed state. This is a relatively large perturbation with each axial layer having a change of roughly 15% in the moderator density. The initial, perturbed, and ETF-predicted cross sections are also shown in Fig. 4. In each case, the cross section was predicted with a high degree of accuracy using the ETF model. The *MAPE* for the predicted absorption, production, and transport cross sections are 0.53%, 0.89%, and 0.22% respectively. Note that the results for the production cross section exclude the reflector region as the cross section is zero in this region for both the initial and perturbed state.

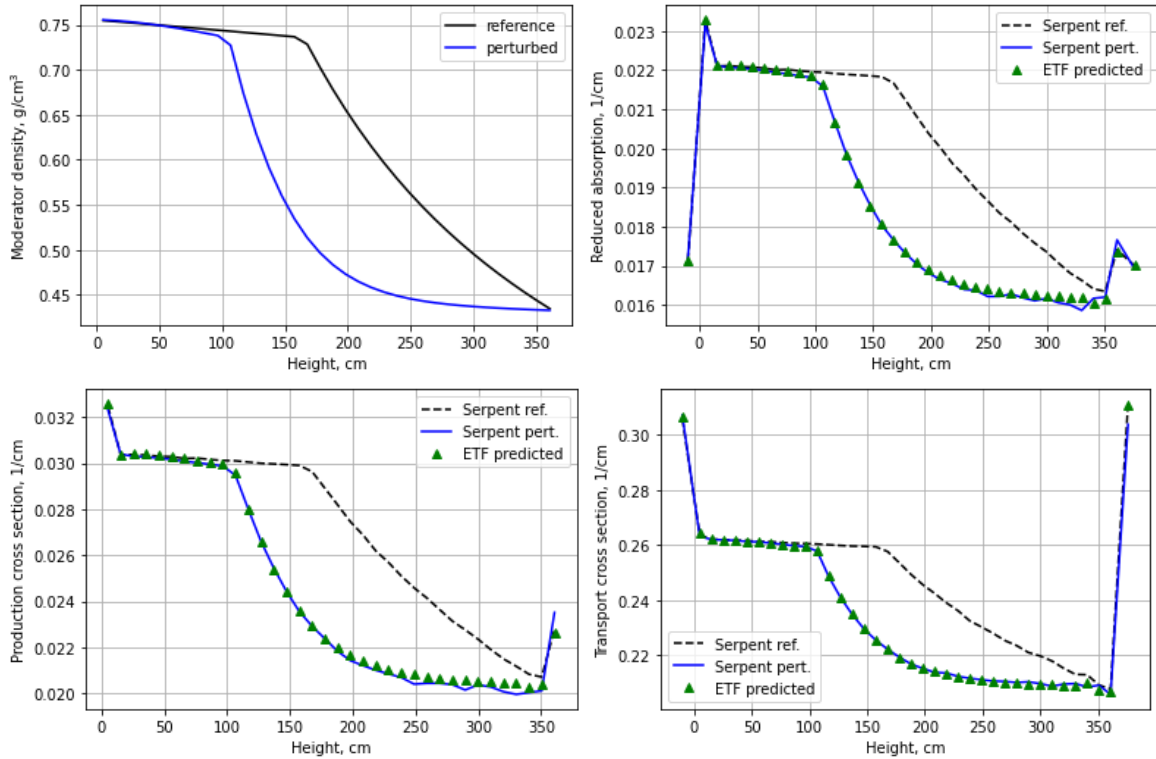


Figure 4. Axially distributed properties. The first row is moderator density (left) and the reduced order absorption cross section (right). The second row is the nu-fission cross section (left) and transport cross section (right)

3.3. Prediction of flux with reference correction factors and predicted cross sections.

The initial and perturbed fluxes obtained by Serpent are shown in Fig. 5 below. The DYN3D prediction was obtained by correcting with the SPH factors (full rank approximation) from section 3.1 and feeding the predicted cross sections from section 3.2.

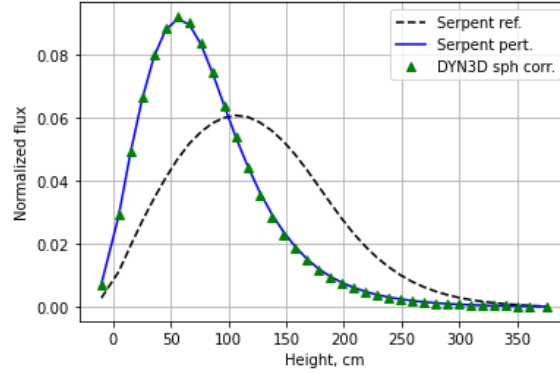


Figure 5. Flux fraction at each axial layer obtained from Serpent and

4. CONCLUSION

Previous work has proposed the use of a prediction block to accelerate coupled MC problems implemented in a PI framework. This prediction block is broken into two sub steps: 1. prediction of cross sections with a linear model and 2. prediction of the flux with a reduced order model using the predicted cross sections. Recent work has demonstrated that flux prediction can be performed quickly using a 1-group nodal diffusion solver. The ETF model has been shown to produce highly accurate cross sections. However, the accuracy of the overall prediction block is still limited by the homogenization error introduced by the nodal diffusion solver. To address this error, this work uses the JFNK method to calculate a set of SPH factors quickly and reliably. It must be stressed that the correction factor calculation, cross section prediction, and flux prediction are executed using only a single MC solution for reference. Further, the computational cost of the entire prediction block is very small compared to the cost of a single MC solution.

ACKNOWLEDGMENTS

This work was supported by funding received from the DOE Office of Nuclear Energy's Nuclear Energy University Program under contract number DE-NE0009218.

REFERENCES

1. B. R. Herman, B. Forget, and K. Smith, “Progress toward Monte Carlo–thermal hydraulic coupling using low-order nonlinear diffusion acceleration methods,” *Annals of Nuclear Energy*, **84**, pp. 63-72 (2015).
2. S. Terlizzi and D. Kotlyar, “On-the-fly prediction of macroscopic cross-section spatial response to the perturbations through transfer functions: Theory and first results,” *Nuclear Science and Engineering*, **194** (4), pp. 280-296 (2020).
3. S. Terlizzi and D. Kotlyar, “A perturbation-based acceleration for Monte Carlo – Thermal Hydraulics Picard iterations. Part I: Theory and application to extruded BWR unit-cell,” *Annals of Nuclear Energy*, **167** (2022).
4. S. Terlizzi and D. Kotlyar, “A perturbation-based acceleration for Monte Carlo – Thermal Hydraulics Picard iterations. Part II: Application to 3D PWR-based problems,” *Annals of Nuclear Energy*, **166** (2022).
5. B. Painter, S. Terlizzi, and D. Kotlyar, “Accelerated Coupled Monte Carlo-Thermal Hydraulic Calculations using a Hybrid GTF-Diffusion-based Prediction Block: First Results,” *Proc. PHYSOR 2022*, Pittsburgh, PA, USA, May 15-20 (2022).
6. B. Painter, V. Lujan, and D. Kotlyar, “Expanded Transfer Function Approach for Predicting Cross Sections due to Thermal Hydraulic Variations with the Shift MG MC Code,” *Proc. ANS Student 2023*, Knoxville, TN, USA, April 13-15 (2023).
7. J. Ortensi et al., “A newton solution for the superhomogenization method: the PJFNK-SPH,” *Ann. Nucl. Energy*, **111**, pp. 579–594 (2018).
8. C. H. Kazaroff, “Validation of plant BUZZ operational data using Serpent-DYN3D sequence,” Master of Science Thesis, Georgia Institute of Technology (2020).
9. B. Painter and D. Kotlyar, “On the use of the Jacobian-free Newton Krylov method to generate equivalence parameters for reduced-order neutron transport,” *Nucl. Sci. Eng. (to be submitted)* (2023).
10. J. Leppänen et al., “The Serpent Monte Carlo Code: Status, Development and Applications in 2013,” *Annals of Nuclear Energy*, **82**, pp. 142 (2015).
11. U. Rohde, V.A. Pivovarov, and Y.A. Matveev, “Studies on boiling water reactor design with reduced moderation and analysis of reactivity accidents using the code DYN3D-MG,” *Kerntechnik*, **77**, pp. 240–248 (2012).
12. A. Kavenoky, “The SPH homogenization method,” *Proc. of a Specialist’s Meeting*, Lugano, Switzerland, Nov. 13-15 (1978).
13. A. Hébert, “A Consistent technique for the pin-by-pin homogenization of a pressurized water reactor assembly,” *Nucl. Sci. Eng.* **113**, pp. 227 (1993).
14. E. E. Y. Shaposhnik and E. Shwageraus, “Thermal-Hydraulic Feedback Module for BGCore System,” *Proceedings of the 25th Conference of Nuclear Societies in Israel*, Dead Sea, Israel (2010).
15. Y. Saad, “A Flexible Inner-Outer Preconditioned GMRES Algorithm,” *SIAM J. Sci. Comput.*, **14**, pp. 461-469 (1993).
16. A. E. Johnson et al., “serpentTools: A python package for expediting analysis with serpent,” *Nuclear Science and Engineering*, **194**, pp. 1016 (2020).